Eur Biophys J (2001) 30: 256–267
DOI 10.1007/s002490000124

ARTICLE

Marcel B.J. Meinders
Geertruida G.M. van den Bosch
Harmen H.J. de Jongh

Adsorption properties of proteins at and near the air/water interface from IRRAS spectra of protein solutions

Received: 25 September 2000 / Revised version: 2 November 2000 / Accepted: 2 November 2000 / Published online: 9 February 2001

Abstract A detailed study is performed using infrared reflection absorption spectroscopy (IRRAS) to characterize the molecular behaviour of proteins at and near the air/water interface of protein solutions. IRRAS spectra of β-casein solutions in H_2O and D_2O show spectral shifts and derivative-like features not commonly observed in monomolecular layer systems. They can be fully understood using optical theory. Fair agreement between experimental and simulated IRRAS spectra over a broad spectral range (4000–1000 cm^{-1}) is obtained using a stratified layer model. An attenuated total reflection and transmission spectrum is used to represent the protein extinction coefficient in H_2O and D_2O, respectively. It is shown that the derivative-like features observed result from the reflective properties of the proteins themselves. Furthermore, both concentration and film thickness could be fitted. At high protein concentrations (100 mg/mL) the spectrum is that of a single homogeneous protein solution. At 0.1 mg/mL, β-casein is accumulated at the surface in a thin layer of approximately 10 nm thickness, with a concentration about 2500 times higher than in the sub-phase. At an initial concentration of 10 mg/mL, the concentration in the surface layer is about 15 times higher than in the sub-phase, while the thickness is about 30 nm.

M.B.J. Meinders (✉) · G.G.M. van den Bosch
H.H.J. de Jongh
Department of Structure and Functionality,
Wageningen Centre for Food Sciences, Diedenweg 20,
Wageningen, The Netherlands
E-mail: marcel.meinders@chem.fdsci.wau.nl
Fax: +31-317-484893

M.B.J. Meinders · G.G.M. van den Bosch
Department of Food Structure and Technology,
ATO Agrotechnological Research Institute,
Bornsesteeg 59, Wageningen, The Netherlands

H.H.J. de Jongh
Department of Food Chemistry, Wageningen University,
Bomenweg 2, Wageningen, The Netherlands

Keywords Infrared reflection absorption spectroscopy · β-Casein · Protein solutions · Air/water interface · Spectral simulation

Introduction

The molecular behaviour of proteins and carbohydrates at interfaces plays a dominant role in the formation and stabilization of colloidal food systems like foams and emulsions. Although it is generally believed that proteins might denature at the air/water interface, it has never been measured directly. Furthermore, very little is known about protein orientation and concentration at the interface and about the ability to form interfacial aggregate networks. This lack of molecular knowledge introduces a lot of uncertainties in the interpretation of the physical phenomena observed in mesoscopic research of food microstructures. Therefore, there is a strong need for experimental methods to study the molecular behaviour of proteins (and carbohydrates) at air/water (A/W) and oil/water (O/W) interfaces. At the same time, system parameters (like surface pressure) as a function of a process (like expanding or compressing surfaces) should be measured. The number of techniques that allow on-line study of the molecular aspects at A/W and O/W interfaces of colloidal solutions is limited. Available techniques to obtain information on the density profile and structure of interfacial molecular layers are specular neutron and X-ray reflectivity (Dickinson et al. 1993a, 1993b; Atkinson et al. 1995, 1996; Berge et al. 1998; Harzallah et al. 1998; Horne et al. 1998; Lu and Thomas 1998; Lu et al. 1998, 1999).

These techniques, however, are not decisive on possible conformational change at the interface. Furthermore, the probing depth is in the order of several nanometers, which is the approximate size of a globular protein, while interfacial films of food relevant proteins may be in the order of micrometers.

Another suitable and possible technique to measure on-line protein molecular characteristics at the A/W

interface of protein solutions, which might overcome the disadvantages mentioned above, is infrared absorption reflection spectroscopy (IRRAS). With this method, the interfacial molecular properties of the proteins are measured by analysing the spectrum of an infrared (IR) beam that is specular reflected at the interface.

IR spectroscopy has already become an important method for molecular characterization of proteins. Attenuated total reflection (ATR) and transmission IR spectroscopy and band shape analysis of the amide I region of absorption spectra have extensively been used to study protein conformations at a detailed (sub-)molecular level in terms of secondary and tertiary structure and their relative orientations (Goormaghtigh et al. 1990, 1994; Jackson and Mantsch 1995; de Jongh et al. 1995, 1997; Bechinger et al. 1999).

Dluhy and co-workers (Dluhy and Cornell 1985; Dluhy 1986; Dluhy et al. 1988) demonstrated that IRRAS is a feasible technique to study the molecular behaviour of lipid monolayers at the A/W interface in a Langmuir balance. Orientation and secondary structure studies of monolayers of proteins, lipids and protein-lipid mixtures have followed this work (Flach et al. 1994, 1996, 1997, 1999; Ren et al. 1994, 1995; Pastrana et al. 1995; Gericke et al. 1997; Baekmark et al. 1999; Wu et al. 1999). Owing to the low signal-to-background ratio, caused by interference of the atmospheric and liquid water (H_2O) with the protein absorption bands, monolayer studies involving proteins are often performed in D_2O. Polarized modulated (PM) IRRAS minimizes the water signal and increases the sensitivity for oriented molecules at the interface. By modulating the polarization of the incoming IR beam, randomly oriented molecules do not contribute to the PM-IRRAS spectrum. Research groups of the University of Bordeaux successfully initiated the application of PM-IRRAS at A/W interfaces (Blaudez et al. 1993, 1994, 1996; Cornut et al. 1996). While PM-IRRAS minimizes the influence of water and is more sensitive for preferred orientations, IRRAS spectra can be used to determine the conformations and concentrations of the proteins.

In contrast to transmission and ATR spectroscopy, where it is generally assumed that the spectra of protein solutions and films is proportional to the extinction coefficient of the proteins, external reflection spectra are complex to analyse. Interpretation of peak positions and intensities is complicated by the reflection properties of the interface. Optical theory can be used to examine the optical effects observed in IRRAS spectra and their influence on peak position and intensities. Several authors have used optical theory to describe IRRAS intensities at a particular frequency and relate these to orientations of lipid chains and protein helices (Ren et al. 1994; Flach et al. 1997, 1999; Gericke et al. 1997), but without simulating the whole IRRAS spectra and including protein and water bands as well. Ulrich and Vogel (1999) used optical theory to simulate PM-IRRAS spectra in the amide I region of lipid/gramicidin monolayers at the A/W interface by simulating the absorption spectrum by a single absorption line. Recently, Buffeteau et al. (1999) obtained good correspondence between experimental and simulated PM-IRRAS of a uniaxially oriented cadmium arachidate monolayer at the A/W interface using experimentally determined optical constants of cadmium arachidate.

In this paper, IRRAS spectra of β-casein solutions are presented for the first time, at a broad range of concentrations, in H_2O as well as D_2O. The spectra show features and spectral shifts in the protein as well as water bands, not commonly observed in IRRAS spectra of monomolecular layer systems. The main focus of this paper is to understand these spectral features using standard optical theory. It is shown that a single layer model is not sufficient to describe the IRRAS data, especially at low protein concentrations. However, the spectral features of the protein as well as water bands are described accurately using the stratified layer model. This understanding allows us to obtain detailed information on protein concentrations, conformations, and possibly also orientations, at and near the A/W interface. This applies not only to monolayer systems, but also to systems having thicker layers and solutions which are of great relevance for chemical physics and related industries, material science, and food science and technology. Although in this work we will focus on the description of interfacial dimensions and protein concentrations, in the near future global analysis fit algorithms will be implemented to obtain information on interfacial protein conformations.

Materials and methods

Fourier transform infrared (FTIR) measurements were performed on a BioRad FTS 6000 spectrometer equipped with a broad band MCT detector. ATR experiments were performed using a ZnSe or Ge crystal (450, trapezoid, six internal total reflections). No clear differences were observed between the spectra collected using a ZnSe or Ge crystal, indicating that the total reflection criteria are met. For the external reflection measurements, an IRRAS accessory (Graceby-Specac, Fairfield, Conn.) was used. The accessory is equipped with a small PTFE Langmuir trough (surface area 10×3 cm, volume 10 mL). The incident and refracting angles of the IR beam can be adjusted continuously from 8° to 85°. The spectrometer was placed on an optical bench table to minimize and dampen external vibrations.

To control the polarization direction of the IR beam on the sample, a grid polarizer, consisting of an aluminium grid deposited on KRS-5, was mounted. The degree of polarization was between 99% (at 10 μm) and 95% (at 3 μm), according to the supplier (Graceby-Specac).

The FTIR spectrometer and compartment were separately purged with a constant flow (approx. 5 L/min) of dry nitrogen gas (5.0N, water content less than 5 Vpm). After closure of the sample compartment, at least 20 min was allowed before recording a spectrum. For the ATR measurements this resulted in spectra of protein films from which the water vapour contribution was not detectable, and no water vapour subtraction was required. For external reflection measurements, however, IRRAS spectra suffered from water vapour contributions, even after equilibration times of more than an hour and subsequent water vapour spectral subtraction. Therefore we developed a device with a movable Langmuir trough, consisting of sample and reference

compartments, replacing the originally mounted Langmuir trough and allowing us to switch automatically between acquisition of the sample or reference spectrum without opening the sample compartment. This reduces the waiting time and water vapour contribution in the IRRAS spectra considerably. However, after subtraction of a water vapour spectrum there still remains a mismatch between the water vapour concentration above the protein solution and above the water phase.

FTIR spectra were acquired from 1000 cm^{-1} to 4000 cm^{-1}. A relatively high spectral resolution of 2 cm^{-1} was used in order to make accurate the subtraction of the water vapour bands. Scans were recorded at 20 kHz scanning speed. The number of scans that was averaged, typically 128, was taken such that an optimum was reached between signal-to-noise ratio and stability of the atmosphere and sample. A triangle apodization function was used and automatic zero filling to a nominal resolution of 2 cm^{-1}. No baseline corrections were performed.

Bovine milk β-casein was obtained from Eurial Poitouraine (Nantes, France). Prior to use, the material was desalted using a PD-10 column (Pharmacia & Upjohn, Peapack, NJ) according to the instructions of the manufacturer.

Protein solutions in H_2O were prepared at different concentrations, ranging from 0.1 mg/mL to 100 mg/mL, in a 20 mM phosphate buffer in H_2O (Millipore, pH 6.8). The β-casein/D_2O solutions were prepared by dissolving different amounts of deuterated β-casein in 99.9% D_2O (pD 6.5). The labile protons of β-casein had been deuterated overnight by dissolution of the protein in excess D_2O and subsequent freeze-drying of the material. It was checked by comparison of the amide I and II bands and by the appearance of the amide II′ band that it was fully amide deuterated.

External reflection spectra were obtained by dividing the measured intensity at a certain angle of incidence with the measured intensity at 90°. At this angle there is no sample between the "incident" and "reflecting" beams and the spectrum corresponds to the optical response of the optical components of the spectrometer and external reflection accessory only. It could be measured by removing the trough, which would otherwise block the IR beam.

It was checked that, during the time period of spectral acquisition, no differences in spectra are observed, indicating that the measurements are performed under equilibrium conditions.

Theory: spectral simulations

The goal of our research is to extract information from external reflection spectra on the protein concentrations, conformations and orientations at the A/W interface and possible differences with respect to the bulk phase. Beside the molecular properties of the proteins, the spectra also depend on optical effects due to reflection properties of the interface. In order to examine these and to be able to distinguish whether or not certain spectral features are due to optical effects or to, for example, a conformational change of the protein, optical theory is used. Optics has already been studied extensively and a review on optical theory applied to IR spectroscopy has been published by Yamamoto and Ishida (1994). For the reader who is not familiar with it, the relevant equations that are used in our calculations are presented below.

The protein molecular properties, being concentration, conformation and orientation, are directly related to the optical properties and are described by the complex refractive index, which is defined as:

$$\hat{n} = n + ik \tag{1}$$

It equals the square root of the dielectric constant ($\hat{\varepsilon} = \hat{n}^2$), and is a function of the wavenumber v. The real part n is the refractive index. The imaginary part k is the extinction coefficient and is related to the absorption coefficient α by $\alpha = 4\pi k/\lambda$, with λ the wavelength of the light. It is the absorption coefficient that is measured in ATR and transmission experiments. Since k depends on the conformation of the proteins, an assessment of the conformation can be made by band shape analysis of the amide I band. The complex refractive index is in general a 3×3 tensor, describing the anisotropy of the material. From this anisotropy, the orientation of molecular bonds can be determined. However, for simplicity and as a start we will assume here that the systems are isotropic, so that $\hat{n}$ can be represented by a scalar.

Reflection or reflection absorption spectroscopy is used to measure the optical properties of proteins at the surface and in the bulk. The reflectivity of a sample $R(v, \theta_0, \mathrm{pol}, \hat{n})$, from now on denoted as R, is measured as the specular reflected light intensity I_R with respect to the incident intensity I_0, yielding $R = I_R/I_0$. It is a function of the wavenumber v and depends on the angle of incidence θ_0, the polarization of the incoming light (pol) and the optical properties of the material $\hat{n}$, in which one is interested.

Often one is interested in the optical response of a sample R with respect to that of a reference R_{ref}. In that case, reflection absorption spectroscopy (RAS) is used, like for example in the study of monolayers or thin films with a solid or liquid substrate as reference. RAS spectra are usually presented as:

$$-\log(R/R_{ref}) \tag{2}$$

In our case the sample is an aqueous protein solution and the reference is water. Experimental data are presented as RAS spectra to be more sensitive for the protein signal because water contributions dominate the spectra of protein solutions.

Reflection spectroscopy

As a first approach we studied the simplest optical configuration in which the protein solution is considered only as a mixture of water and proteins, neglecting possible surface activity. In this case the optical configuration consists of a single interface between air and solution, as schematically shown in the left panel of Fig. 1.

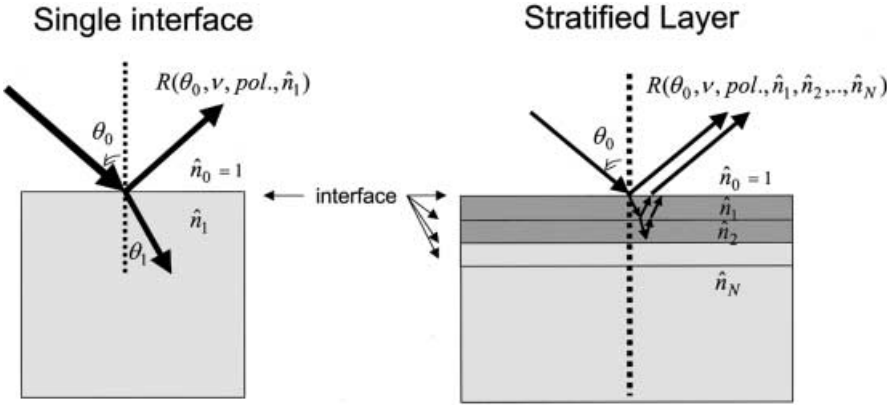

Fig. 1 Schematic view of the optical configuration of a single reflecting interface (*left*) and that of the stratified layer (*right*). The reflectivity R is a function of the incidence angle θ_0, the complex refractive index of layers $\hat{n}_j$, of the polarization direction of the light (pol) and of the wavelength v. The incidence medium is air ($\hat{n}_0 = 1$)

The complex refractive index can be determined from the external reflection spectrum R, using the Kramers-Kronig relationship between the logarithm of the reflection spectrum and the phase shift between incident and reflected beams. This analysis is widely used and has been published elsewhere (Bardwell and Dignam 1985), while here we only show the relevant equations.

The complex reflection coefficient $\hat{r}$ can be written as:

$$\hat{r} = R^{1/2} e^{i\phi} \tag{3}$$

where ϕ is the phase shift. According to Fresnel, the reflection coefficient for an optical configuration with only one reflecting surface and for s-polarization (polarization direction of the light is perpendicular to the plane of incidence), is given by:

$$\hat{r} = \frac{\hat{n}_0 \cos\hat{\theta}_0 - \hat{n}_1 \cos\hat{\theta}_1}{\hat{n}_0 \cos\hat{\theta}_0 + \hat{n}_1 \cos\hat{\theta}_1} \tag{4}$$

where $\hat{n}_0$ and $\hat{n}_1$ are the refractive indices of the incidence and reflecting medium, respectively, while $\hat{\theta}_0$ and $\hat{\theta}_1$ are the angles of incidence and refraction, respectively (see Fig. 1). Schnell's law relates the refractive indices and angles by:

$$\hat{n}_0 \sin\hat{\theta}_0 = \hat{n}_1 \sin\hat{\theta}_1 \tag{5}$$

From Eqs. (4) and (5), $\hat{n}_1$ can be solved, yielding:

$$\hat{n}_1 = \hat{n}_0 \left(\sin^2\hat{\theta}_0 + \left(\frac{\hat{r}-1}{\hat{r}+1}\right)^2 \cos^2\hat{\theta}_0 \right)^{1/2} \tag{6}$$

In our case the incidence medium is air, giving $\hat{n}_0 = n_0 = 1$ and $\hat{\theta}_0 = \theta_0$ are real. Furthermore, the refractive index of the protein solution $\hat{n}_1$ is larger than that of air, so we are in the external reflection regime. In that case, the Kramers-Kronig relationship between the reflectivity R and the phase shift ϕ is given by:

$$\phi(\nu) = \frac{2\nu}{\pi} \int_0^\infty \frac{\ln R^{1/2}(\nu')}{\nu'^2 - \nu^2} \, d\nu' \tag{7}$$

where ν and ν' are the wavenumbers.

Using Eqs. (3), (6) and (7), the complex refractive index of the protein solution $\hat{n}_1$ can be determined from its reflection spectrum $R(\nu)$. In this work, the reflectivity spectrum was measured between 1000 and 4000 cm^{-1} and McLaurin's formulae were used for the calculation of the Kramers-Kronig transformation (KKT) (Ohta and Ishida 1988).

It is assumed that the extinction coefficient of the protein solution $k_{mix}(\nu) = k_1(\nu)$ is given by $k_{mix} = (1-x)k_w + xk_{prot}$, where $k_w(\nu)$ is the extinction coefficient of water, x the protein concentration and $k_{prot}(\nu)$ the extinction coefficient of the protein. The extinction coefficient of the water is calculated from the water reflection spectrum. The extinction coefficient of the protein $k_{prot}(\nu)$ is assessed by subtracting a scaled amount of $k_w(\nu)$ from $k_{mix}(\nu)$ in such a way that an as good as possible representative protein absorption spectrum was obtained, essentially free of water contributions.

Stratified layer model

To obtain insight into the molecular properties at the surface and at different depths, computer algorithms for the spectral simulation of multilayer systems were also developed.

In the right panel of Fig. 1 the optical configuration is shown of such a stratified medium, which consists of $N+1$ homogenous plane-parallel layers (N interfaces), including the incidence medium which is layer 0; layer N is the substrate or reference. The optical properties of each layer are described by the complex refractive indices. For layer j it is defined as $\hat{n}_j = n_j + ik_j$.

The reflectivity of the stratified layer can be calculated using an iteration procedure and Fresnel equations for transmission and reflection, as described above. However, Abeles developed an elegant matrix formalism to calculate the reflectivity for stratified layers. The theory has already been published in many papers and textbooks (e.g. see Born and Wolf 1975) and is also commonly applied in (spectral) ellipsometry, X-ray and neutron reflectometry to determine layer thickness, density profiles and optical parameters (Yamamoto and Ishida 1994). Here we only present the relevant equations used in the computer algorithms.

In the derivation of the matrix formalism it is assumed that the phase coherence remains between the multiple reflected and transmitted light beams at the different interfaces between different layers. Therefore, the amplitudes are added coherently, which is usually the case when dealing with thin homogeneous layers. In that case the reflection coefficient of the stratified layer system is given by:

$$r = \frac{(m_{11} + m_{12}g_N)g_1 - (m_{21} + m_{22}g_N)}{(m_{11} + m_{12}g_N)g_1 - (m_{21} + m_{22}g_N)} \tag{8}$$

where the m's and g's are defined below. Labels for polarization, incoming angle and wavenumber have been omitted for clarity.

The m's in Eq. (8) are the four elements of a 2×2 characteristic matrix, M, of the stratified layer. It is the product of the characteristic matrix, M_j, of each layer j, and is defined as:

$$\begin{aligned} M &= \begin{pmatrix} m_{11} & m_{12} \\ m_{21} & m_{22} \end{pmatrix} = M_1 M_2 \ldots M_{N-1} = \prod_{j=1}^{N-1} M_j \\ &= \prod_{j=1}^{N-1} \begin{pmatrix} \cos\beta_j & -\frac{i}{g_j}\sin\beta_j \\ -ig_j \sin\beta_j & \cos\beta_j \end{pmatrix} \end{aligned} \tag{9}$$

For s-polarization the parameters are given by:

$$g_{j,s-pol} = \hat{n}_j \cos\hat{\theta}_j \tag{10}$$

$$\beta_{j,s-pol} = 2\pi\nu d_j g_{j,s-pol} \tag{11}$$

while for p-polarization, with its electric field directed in the plane of incidence, the parameters are given by:

$$g_{j,p-pol} = \frac{\cos\hat{\theta}_j}{\hat{n}_j} \tag{12}$$

$$\beta_{j,p-pol} = 2\pi\nu d_j \hat{n}_j^2 g_{j,p-pol} \tag{13}$$

where d_j is the thickness of layer j. Schnell's law ($\hat{n}_0 \sin\hat{\theta}_0 = \hat{n}_j \sin\hat{\theta}_j$) defines the complex refractive angle $\hat{\theta}_j$ in layer j. Here $\hat{n}_0 = 1$ and $\hat{\theta}_0 = \theta_0$ is the angle of incidence.

Contrary to the simple optical configuration of a single reflecting interface, it is not possible in the case of the stratified layer model to express the complex refracting indices in terms of the reflectivity. Therefore, iteration and fit procedures must be used to determine the unknown parameters d_j and $\hat{n}_j$.

Our first and main concern is to understand the IRRAS spectra of protein solutions. In order to distinguish between optical effects and protein molecular properties present in the spectra, we simulated IRRAS spectra using an ATR spectrum of a dried protein film as a measure of the extinction coefficient k_{prot} of the protein (apart from proportionality constant), for the H_2O solutions. The optical constants $\hat{n}_w = n_w + ik_w$ of water (H_2O and D_2O) were taken from the literature (Bertie et al. 1989). For the D_2O system the transmission spectrum of deuterated β-casein was used to represent the imaginary part of the complex refractive index.

The real part of the complex refractive index can be calculated from the imaginary part using the Kramer-Kronig relation:

$$n(\nu) = n(\infty) + \frac{2}{\pi} \int_\pi^\infty \frac{\nu' k(\nu')}{\nu'^2 - \nu^2} \, d\nu' \tag{14}$$

where $n(\infty)$ is the baseline refractive index. From a refractometer study in the visible region, we experimentally determined the refractive index n_{mix} of β-casein solutions at different concentrations

c (results are not shown). A linear relation up to saturated concentration was found:

$$n_{\mathrm{mix}} = n_{\mathrm{w}} + \eta_c \tag{15}$$

where $n_{\mathrm{w}} = 1.332$ is the refractive index of water in the visible region, c is the protein concentration in mg/mL and $\eta = \Delta n/\Delta c = 1.8\times10^{-4}$ ml/mg. This value is common for most proteins (de Feijter et al. 1978).

For the determination of the complex refractive index of the protein mixture, first the extinction coefficient of the solution k_{mix} is calculated, using:

$$k_{\mathrm{mix}} = v_{\mathrm{w}}k_{\mathrm{w}} + v_{\mathrm{prot}}k_{\mathrm{prot}} \tag{16}$$

where $v_{\mathrm{prot}} = v_{\mathrm{p}}c$ and $v_{\mathrm{w}} = 1 - v_{\mathrm{prot}}$, with v_{p} the partial specific volume [which is in the order of 7×10^{-4} mL/mg for most proteins (Creighton 1996)].

The real part of the refractive index of the mixture is calculated using the KKT (Eq. 14). For its value at infinite wavenumber we used Eq. (15).

The fit parameters are now the proportionality constant relating the protein ATR/absorption spectrum and the protein extinction coefficient k_{mix}, the number of layers N, the concentration of the protein c_j for each layer, and thickness d_j of the layers above the substrate ($1 \le j < N$). It is noted that for protein solutions the substrate need not necessarily be water, but can also be a protein solution. Currently, the IRRAS spectra are fitted by hand, but software is under development containing global analysis iterative fit procedures to extract the extinction coefficient of the proteins at the interface and using an ATR and/or transmission spectrum as a first estimate.

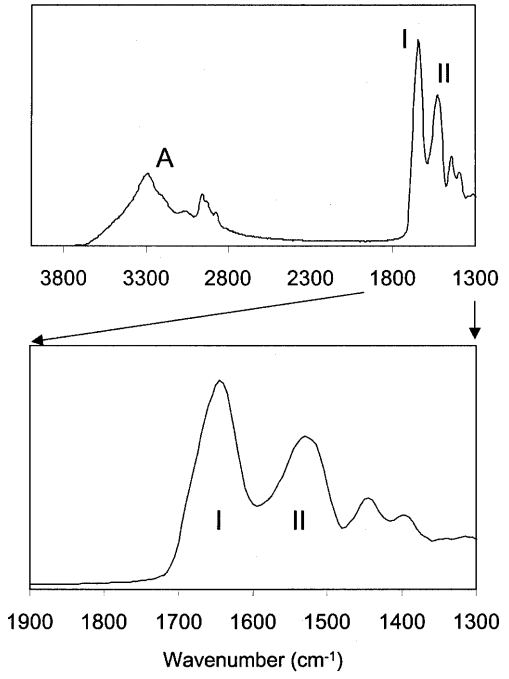

Fig. 2 Infrared ATR spectrum (Ge crystal) of a β-casein film, dried from 100 µL β-casein solution (20 mg/mL in 20 mM phosphate/H_2O buffer). Amide bands A, I and II are indicated. The *lower panel* shows the amide I and II region

Results

Experiments

In Fig. 2 an ATR spectrum (using a Ge crystal) of a β-casein film, dried from 100 µL β-casein solution (20 mg/mL in 20 mM phosphate/H_2O buffer) is shown. The upper panel displays the protein absorption spectrum from 4000 cm^{-1} to 1300 cm^{-1}, while in the lower panel the amide I region is shown. The amide A peak position is located at 3300 cm^{-1}. The amide I band is located between 1595 and 1710 cm^{-1}, with the maximum at 1645 cm^{-1}, corresponding to the random coil conformation of the protein (Byler and Susi 1986). The maximum of the amide II band is at 1528 cm^{-1}.

In Fig. 3 (upper panel), typical external reflection spectra are shown of an A/W interface. The thick and thin curves correspond to the external reflection spectra of an H_2O reference sample (20 mM phosphate/H_2O buffer) (R_{ref}) and to a 10 mg/mL β-casein solution (R), respectively. Figure 3 shows the derivative-like spectral features, typical for external reflection spectroscopy. The feature at 3300 cm^{-1} corresponds to the O-H stretching mode of water and that at 1650 cm^{-1} to the O-H bending mode. It can be seen that the external reflection spectrum of the protein solution is strongly dominated by the water bands. On the average, approximately 2% of the intensity is reflected, as can be seen in Fig. 3. This is in agreement with the theoretical value, as can be calculated using the Fresnel Eq. (4). Dividing both spectra and taking the logarithm, according to Eq. (2) yields the IRRAS spectrum of the 10 mg/mL β-casein solution,

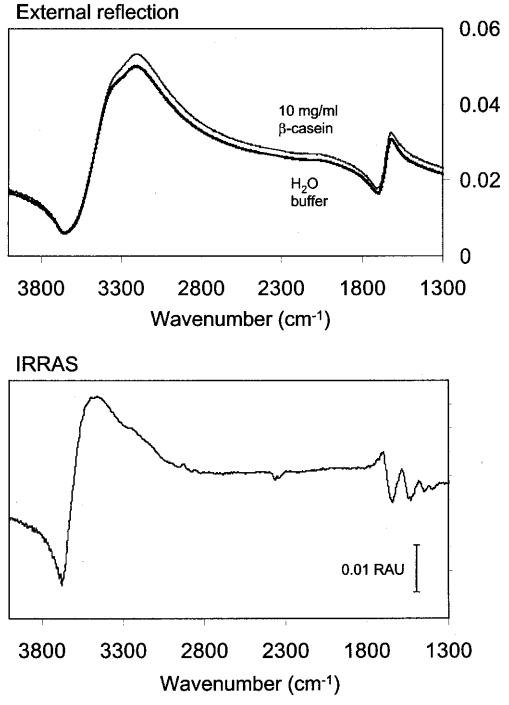

Fig. 3 *Upper panel*: external IR reflection spectra of phosphate/H_2O buffer (R_0, *thick line*) and that of a 10 mg/mL β-casein solution in a phosphate/H_2O buffer (R, *thin line*). *Lower panel*: IR reflection absorption spectrum of the β-casein solution ($-\log R/R_0$). Spectra are collected using s-polarization and a 30° angle of incidence

which is shown in the lower panel of Fig. 3. The feature at 3500 cm^{-1} is descended from a different optical response of the O-H stretching mode between the water and protein solutions. At its slope at the low wavenumber side, the amide A band is observed around 3200 cm^{-1}. Because the peak position and band shape from the amide I band can be interpreted in terms of conformation at a secondary level, we are especially interested in the amide I region of the spectrum.

In Fig. 4, IRRAS spectra of the amide I region of a 10 mg/mL β-casein solution in 20 mM phosphate/H_2O buffer at different angles of incidence θ_0 are shown for s-and p-polarization. The IRRAS spectra are corrected for water vapour contributions, by subtracting a water vapour spectrum that was acquired by opening the sample compartment briefly.

The amide I and II bands, pointing downwards, can clearly be distinguished in the region between 1410 and 1700 cm^{-1}. For s-polarization, no differences than lower intensity with increasing angle of incidence are observed. The intensity of the amide I reflection-absorption band, measured between its maximum and minimum, decreases for s-polarization from 0.014 reflectance-absorbance units (RAU) at 10° to 0.005 RAU at 70° incidence angle.

For p-polarization, the intensity of the amide I band increases from 0.015 RAU at 10° incidence to 0.03 RAU at 50°. Near the Brewster angle (around 55°), where the reflectivity of the p-polarized light goes to zero, the signal-to-noise ratio increases, while for incidence angles larger than the Brewster angle, amide II flips its orientation from downwards to upwards. This behaviour of the intensity variation with incidence angle is quite common for monolayer studies and has been observed in the methylene and carbonyl stretching vibration bands of lipids on dielectric substrates (Ren et al. 1994; Flach et al. 1997; Blaudez et al. 1998). For angles larger than the Brewster angle, no clear amide I band can be observed any more, but it seems to be obscured by the dispersion of the water refractive index near the strong H_2O bending mode at 1640 cm^{-1}.

The maxima of the amide I and II bands are located at approximately the same position, as measured with the ATR. However, the spectra show a strong positive feature at 1700 cm^{-1}, near the amide I band. This results in a derivative-like amide I feature and a change or distortion in band shape with respect to the ATR spectrum.

Similar features have also been observed before in IRRAS monolayer studies on H_2O, but are still not well understood (Dluhy and Cornell 1985; Gericke and Hühnerfuss 1993; Simon-Kutscher et al. 1996; Flach et al. 1997). The features either remain unexplained, are attributed to interfacial structured water and/or hydration water bound to the protein, or alternatively to the dispersion of the water refractive index. From the presence of the large derivative feature at the position of the water stretching mode around 3500 cm^{-1} in the IRRAS spectrum displayed in Fig. 3, it may be expected that water contributions are present also in the amide I region. PM-IRRAS spectra of oriented monolayers display similar features (Buffeteau et al. 1999; Ulrich and Vogel 1999). Recently, Buffeteau et al. (1999) ascribed these, based on spectral simulations, to a difference in optical response of water surfaces with or without a monolayer, and maybe partly to structured water. However, the features are still not well understood and to interpret IRRAS spectra in terms of secondary structure, the shape of this positive feature under the amide I region needs to be quantified. As an alternative, measurements could be performed in D_2O. If the features are due to interference with the H_2O bending mode, they shift to the region of the deuterium bending mode which is located at 1200 cm^{-1}.

In order to understand the origin and to quantify the shape of the positive feature at 1700 cm^{-1}, we performed IRRAS experiments on different concentrations of β-casein solutions in D_2O, ranging from 100 mg/mL (Fig. 5, top spectrum) to 1 mg/mL (lowest spectrum).

The spectra clearly show similar positive features at 1700 cm^{-1} for protein solutions having high concentrations, as in the H_2O case. This indicates that these are not due to structured water or a different optical response of the water bands, but must be attributed to the proteins. The ratio of the amide I and II bands, and of the appearance of the amide II′ band near 1450 cm^{-1}, indicates that β-casein has been completely deuterated. The figure also shows that the height of the feature at 1700 cm^{-1} gradually disappears on going from high to low protein concentrations. At a concentration of 100 mg/mL the height is 0.03 RAU, while at 1 mg/mL no positive feature can be observed any more. It is noted that if all proteins

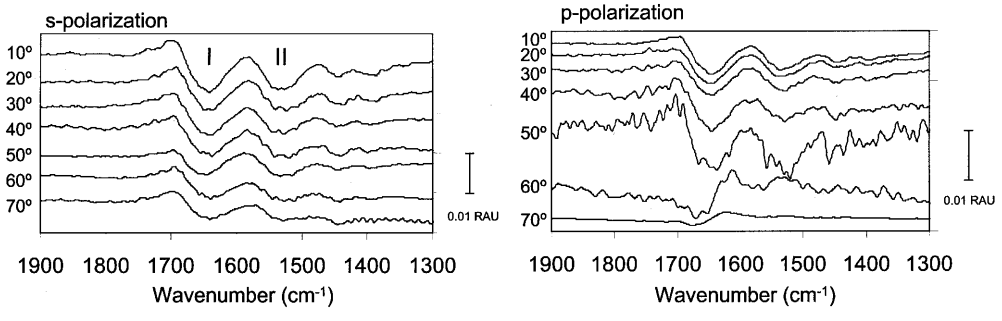

Fig. 4 IRRAS spectra of the amide I region of a 10 mg/mL β-casein solution in 20 mM phosphate/H_2O buffer at different angles of incidence θ_0 (indicated), using s-polarization (*left*) and p-polarization (*right*). Amide I and II bands are indicated. An offset has been added to the spectra for clarity

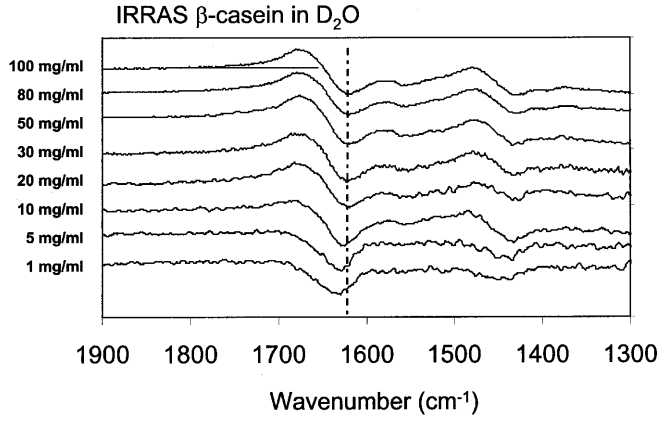

Fig. 5 IRRAS spectra of the amide I region of β-casein solutions in D_2O having different concentrations (as indicated). The spectra are collected at a 30° angle of incidence, using s-polarization, and are scaled and provided with an offset for clarity

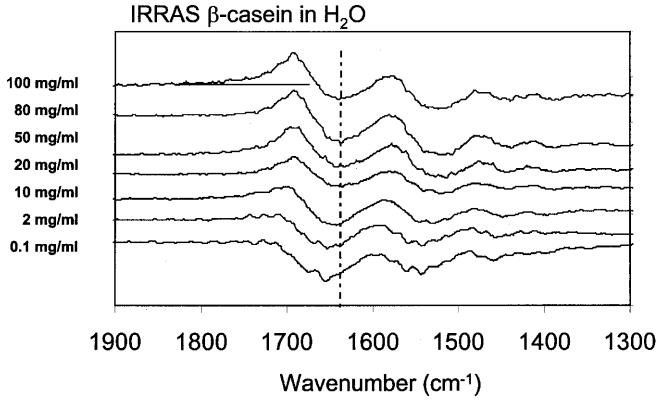

Fig. 6 IRRAS spectra of the amide I region of β-casein solutions in phosphate/H_2O having different concentrations (as indicated). The spectra are collected at a 30° angle of incidence, using s-polarization, and are scaled and provided with an offset for clarity

would accumulate at the interface, a monolayer of β-casein would require a concentration of approximately 10 μL/mg for the Langmuir trough we used. The peak position of the amide I band for the 100 mg/mL solution is located at 1620 cm^{-1}, which is quite unusual for a random coil protein dissolved in D_2O (Byler and Susi 1986; Goormaghtigh et al. 1994). Whether or not this is due to a protein conformational change or optical effects is not clear at this point. The peak is shifted to 1632 cm^{-1} for the β-casein solution having a concentration of 1 mg/mL, which is a more usual position in D_2O. Similar behaviour can also be observed at the amide II′ band, where at high protein concentrations of 100 mg/mL a positive feature is seen at 1478 cm^{-1} while the amide II′ peak is located at 1427 cm^{-1}. At low concentrations this positive feature at 1478 cm^{-1} is not observed, while the amide II′ peak is shifted to 1445 cm^{-1}.

At this point the spectral features observed in IRRAS spectra are not well understood and IRRAS results cannot be interpreted in a straightforward manner, as has been suggested by Picard et al. (1999). It is not at all clear whether the observed shifts in peak positions are due to conformational changes of the protein or are a result of optical effects. It is therefore of crucial importance that the origin of the derivative features are understood and can be quantified in order to be conclusive on the conformation.

We also performed a similar IRRAS study on different concentrations of β-casein dissolved in 20 mM phosphate/H_2O buffer. The spectra are displayed in Fig. 6 and clearly show similar behaviour of the derivative features as a function of concentration, as observed in the D_2O study (Fig. 5). The height of the positive feature at 1700 cm^{-1} diminishes from 0.03 RAU for protein solutions having a high concentration of 100 mg/mL to zero for the solution of 0.1 mg/mL. The location of the peak position of the amide I band shifts from 1637 cm^{-1} for the 100 mg/mL solution to approximately 1655 cm^{-1} for the 0.1 mg/mL β-casein solution.

Spectral calculations

Reflection spectroscopy

As demonstrated above, spectral calculation is necessary in order to conclude about protein conformation on the basis of the shape and position of the amide I band and rule out possible optical effects. From external reflection spectra R, the complex refractive indices $\hat{n}$ can be calculated using Eqs. (3), (6) and (7). In Fig. 7, results are shown for a 10 mg/mL β-casein solution in a phosphate/H_2O buffer, calculated from the external reflection spectra shown in Fig. 3. In the left panel of Fig. 7 the calculated extinction coefficients of the protein solution k_{mix} and that of the protein free buffer k_w are shown. We omitted the real part of the complex refractive index. Using $k_{prot} = (k_{mix} - (1 - x)k_w)/x$, the extinction coefficient of the protein is assessed by subtracting a scaled amount [equal to $(1 - x)$], of k_w from k_{mix}, in such a way that an absorption spectrum was obtained with a band shape that compared as good as possible (minimal mean squared error) with the representative β-casein absorption spectrum (shown in Fig. 2). The best estimate of the extinction coefficient of β-casein k_{prot} was obtained for $x = 0.06$. This result is shown in the right panel of Fig. 7. Deviations of x of more than 0.005 result in spectra clearly showing water bands at 3200 and 1650 cm^{-1}. As can be seen in the right lower panel of the figure, amide I and II bands can be observed. The signal-to-noise ratio is poor because noise levels due to water vapour contributions and imperfections in the alignment are enlarged by the spectral manipulations. However, there are still large water-like contributions present, as can be seen from the features around 3000 cm^{-1} that cannot be attributed to amide A vibrations only. It is noted that the optical constants of the protein obtained using ATR (dried film) will most probably not be exactly equal to that of the protein in solution. However, this could never explain the observed differences, indicating that the single layer formalism is not appropriate to describe the

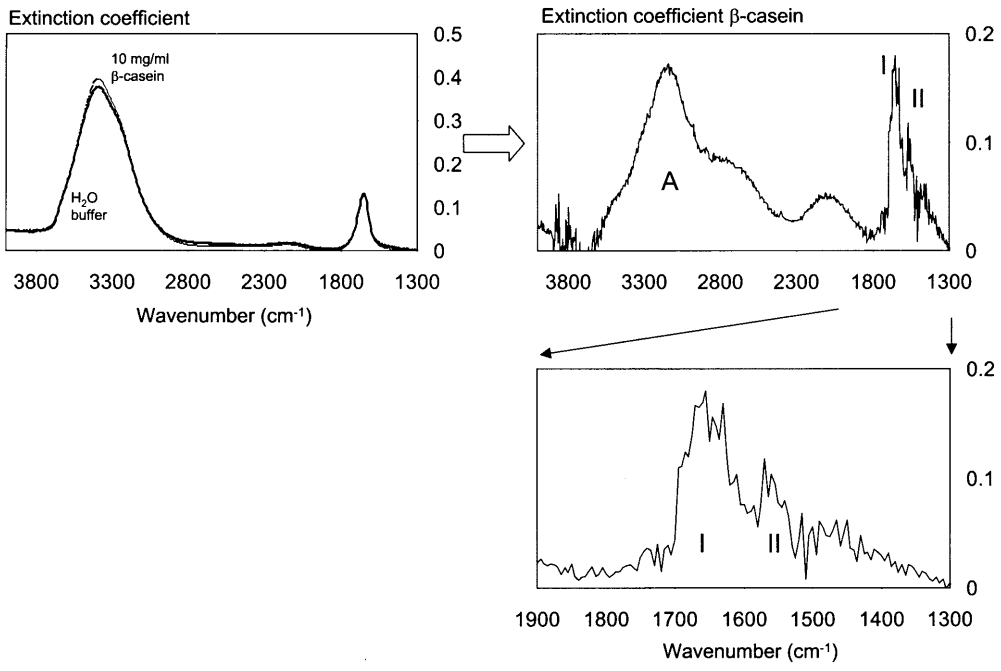

Fig. 7 Left: extinction coefficient of a 10 mg/mL β-casein solution in phosphate/H_2O buffer (k_{mix}, *thin line*) and of the reference buffer (k_w, *thick line*), as calculated from external IR reflection spectra collected at a 30° incidence angle and s-polarization (Fig. 3). *Right*: calculated extinction coefficient of β-casein: $k_{prot} = (k_{mix} - 0.94k_w)/0.06$. In the *lower right panel*, an enlargement of the amide I region is shown. Amide A, I and II regions are indicated

system. This observation holds for much better signal-to-noise ratios of the amide I band that is also broadened owing to the presence of water-like features. From similar calculations of β-casein solutions at different concentrations it turned out that for lower protein concentrations the results were even worse. No representative protein spectrum, with comparable band shape as the β-casein absorption spectrum (Fig. 2), could be obtained by simply subtracting the water extinction coefficient from that of the protein solution (results not shown). It is concluded that the calculation of the protein extinction coefficient from reflection spectra in the simple optical configuration of one reflecting surface is not appropriate and that multilayer systems should be considered.

Spectral simulations using the stratified layer model

In order to understand the spectral features observed in the IRRAS spectra of β-casein solutions of different concentration (H_2O as well as D_2O), and in order to distinguish between optical effects and protein molecular properties present in the spectra, we performed spectral simulation calculations using the stratified layer model. An ATR spectrum of a dried film of β-casein dissolved in a phosphate/H_2O buffer (Fig. 2) is used as the extinction coefficient of hydrated β-casein, apart from a proportionality factor. For the extinction coefficient of deuterated β-casein, a scaled transmission spectrum of a 20 mg/mL β-casein in D_2O solution, placed in a 34 μm cuvette, is used. The extinction coefficients of H_2O and D_2O were taken from the literature (Bertie et al. 1989).

The fit parameters in the spectral simulation calculation are the proportionality constant mentioned above, the number of layers of the stratified layer model, the protein concentration in each layer and the thickness of the layers above the substrate. For the (baseline) refractive index of the protein solution at infinite wavelength, we used Eq. (15).

In Fig. 8 we show experimental and simulated IRRAS spectra of β-casein solutions in H_2O (left panel) and D_2O (right panel) having different concentrations (as indicated). The lower panels show an enlargement of the amide I region. The spectra are fitted by adjusting the parameters by hand. It can be seen that the experimental IRRAS spectra agree well with the simulation; not only the protein bands show good resemblance but also the water features do. The observed discrepancies in the amide II region may be due to the differences in optical constants between that of a dry protein film and that of a fully hydrated protein in solution. This shows that the observed uncommon spectral shifts and derivative-like features can be understood by considering the optical effects caused by the external reflection only, without considering protein conformational changes.

Fit parameters

Proportionality constant

The proportionality constant is an arbitrary constant to scale the experimental protein absorption to its extinction coefficient and is dependent on the protein concentration, film quality, cell length, etc. The proportionality constant turned out to be such that the maximum value of the β-casein extinction coefficient of the amide I peak is in the order of 0.4–0.6. This is comparable to values reported in literature, which are

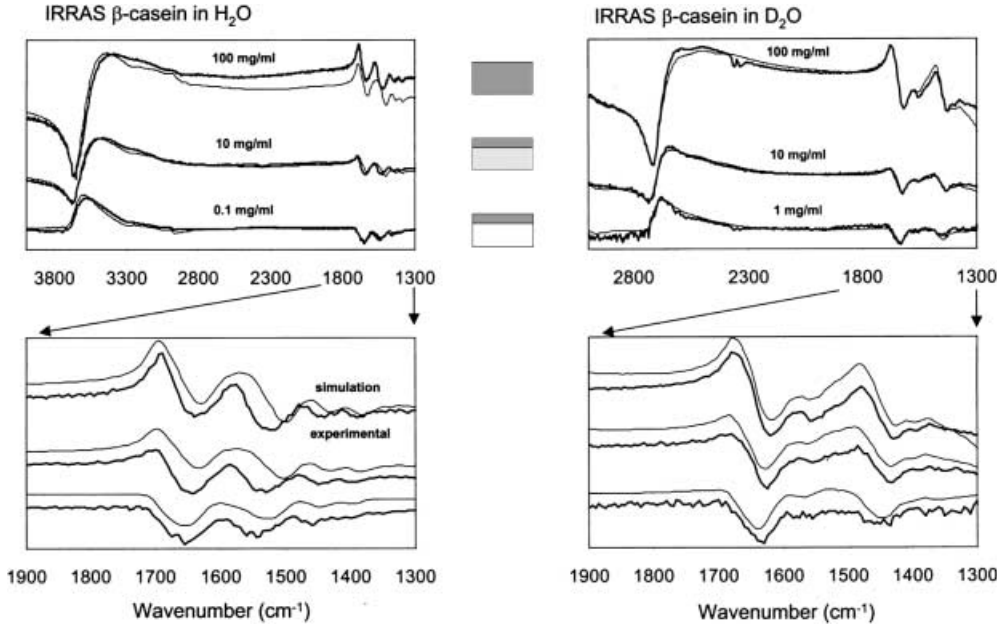

Fig. 8 Experimental (*thick lines*) and simulated (*thin lines*) IRRAS spectra of β-casein solutions in phosphate/H_2O (*left*) and in D_2O (*right*) having different concentrations. In the *two lower panels* an enlargement of the amide I region is shown (an offset is added for clarity). The protein concentrations are indicated as well as a schematic view of the layer model coming out of the spectral simulations (shown between upper-left and upper-right panels). The *lowest curves* correspond to 0.1 mg/mL (in H_2O) and 1 mg/mL (in D_2O) solutions. At these low concentrations the protein system can be viewed as a concentrated single layer on water substrate. The *middle curves* correspond to a 10 mg/mL solution, which can be viewed as a concentrated layer on an approximately 10 times less concentrated protein solution. The *top curves* correspond to a 100 mg/mL solution, which can be modelled by a single reflecting surface

obtained by fitting the amide I peak maximum as a function of angle of incidence and polarization to determine the orientation of protein helices (Gericke et al. 1997; Flach et al. 1999).

Number of layers in the stratified layer model

For the highly concentrated β-casein solution (100 mg/mL, top spectra), the simulations show that a single reflecting interface describes the system well. For intermediate concentrations (10 mg/mL, middle spectra) and low concentrations (0.1 and 1 mg/mL, lowest spectra), good fits were obtained using a single layer on top of a homogeneous bulk phase. These are the simplest models that already described the experimental IRRAS spectra well. It is not possible to describe, for example, the 0.1 mg/mL and 1 mg/mL protein solutions by the single layer model. Simulated IRRAS spectra using a single layer model always shows the positive feature at 1700 cm^{-1} and the sharp feature, pointed downwards, near 3700 cm^{-1} (H_2O) or 2700 cm^{-1} (D_2O). These features are not observed in the experimental IRRAS spectra at low initial concentrations.

Protein concentration in each layer and thickness of the layer above the sub-phase

The IRRAS spectra of the highly concentrated system can be described by a homogeneous protein solution of 100 mg/mL. At intermediate β-casein concentrations (10 mg/mL), a single top layer is formed having a concentration approximately 10–20 times higher as that in the homogeneous bulk phase (10 mg/mL). The thickness of the layer is in the order of 20–50 nm. At low concentrations (0.1 and 1 mg/mL), the simulations also indicate that a highly concentrated β-casein surface layer is formed, having a thickness about 5–15 nm. The protein concentration in the surface layer is about 2000–3000 and 200–300 times higher as in the sub-phase for the 0.1 mg/mL and 1 mg/mL protein solutions, respectively. The concentration values found are of the same order of magnitude, although somewhat smaller, than the β-casein micelle concentration (about 360 mg/mL). Summarizing: increase of the initial protein concentration results in an increase of surface layer thickness and a decrease of the difference in concentration between surface layer and bulk substrate, going to zero for high concentrations.

The values mentioned have that large error margin due to the fact that only one IRRAS spectrum is considered and that the deduced values of the surface layer thickness and concentration to obtain a best fit are not independent. This means that for the 1 mg/mL solution, for example, a layer thickness of 15 nm and a concentration ratio of about 200 yields a similar best fit as the simulation with a layer thickness of 5 nm and a concentration ratio about 300. Currently we are developing

software to analyse IRRAS spectra at different angles of incidence and polarization in order to refine the fit and obtain unique fit results that will reduce these uncertainties.

Values found for the thickness of the accumulated layer are similar to those found in X-ray and neutron reflection experiments (Dickinson et al. 1993a, 1993b; Harzallah et al. 1998). Experiments on β-casein solutions (concentrations between 10^{-4} and 1 mg/mL) could be well fitted using a model consisting of two concentrated surface layers, with a total thickness about 9 nm, on top of a protein-free sub-phase. The thickness of the first (top) layer is about 2 nm and has a protein volume fraction of 0.94, while the second layer has thickness of 7 nm and protein volume fraction of 0.2. X-ray and neutron reflection are sensitive techniques to determine density profiles up to a depth in the order of 10 nm. However, the probing depth of IRRAS is much larger and is in the order of 1–2 μm. This is based on the fact that signals reflected at an interface 2 μm beneath the A/W surface have approximately 0.5% of their original intensity and could easily be detected.

Discussion

The spectral shifts of the amide I band and the height of the feature at 1700 cm^{-1} are reproduced well by the simulations, as can be seen in the lower panels of Fig. 8. In the case of protein solutions in D_2O, the derivative-like features are due to the dispersion of the protein refractive index. For H_2O solutions, also a water contribution in the amide I is present owing to a different reflectivity of the water O-H bending mode between protein-free and solvent water. The differences in optical response of the water O-H stretching modes find expression in the large derivative features at 3500 cm^{-1} (H_2O solution) and 2700 cm^{-1} (D_2O solution).

For the D_2O system, the whole amide I and II′ region is simulated very well. The same holds for the amide I band of the H_2O system. The top of the amide II band for the H_2O system, however, appears at lower wavelength in the simulations, as observed experimentally. This could be due to the difference in optical constants between that of the dry film, which was taken as input of the calculation, and that of the protein in solution.

The simulations are sensitive to the thickness of the surface layer and to the protein concentration difference between the surface layer and the sub-phase. Besides the amide I region, information is also present in the water features that result from a difference in optical response of the O-H and O-D bending modes at 3500 cm^{-1} and 2900 cm^{-1}, respectively, between the sample and reference. Taking this information also into account makes IRRAS in combination with spectral simulation a powerful tool for the determination of the molecular behaviour of proteins or biomolecules at and near the A/W interface, not only for monolayer systems but also for systems having thicker layers and solutions. Especially the latter systems are of great relevance, for example for food science and technology, material science, and chemical physics and related industries. Here we have demonstrated that IRRAS in combination with spectral simulation can yield concentrations of an accumulated protein layer, its thickness and also the protein concentration in the bulk.

Conclusion

We present here, for the first time, IRRAS spectra of solutions of β-casein at different concentrations in H_2O as well as D_2O. It is demonstrated that the observed spectral shifts and derivative-like features in the amide I region (not observed in monolayer studies) can be fully understood using spectral simulations and are mainly due to the dispersion in the refractive index of the protein itself. Using a β-casein absorption spectrum as a measure for the protein extinction coefficient, fair resemblance was obtained between experimental and simulated IRRAS spectra over a broad spectral range (4000–1000 cm^{-1}). Highly concentrated β-casein solutions behave like a single bulk phase, while for intermediate and low concentration a surface layer on top of a homogeneous bulk phase is formed. The concentration difference between the surface layer and the sub-phase decreases when the initial protein concentration increases. The thickness of the surface layer increases with protein concentration and is comparable to that found using alternative techniques such as X-ray and neutron reflection.

The spectral simulation in comparison with experiments, over the broad spectral range, gives a better understanding of the optical effects present in experimental external reflection (absorption) spectra and allows the determination of the optical properties of the system of interest. It has been shown that it can yield information about protein concentrations in an accumulated layer, the thickness of the layer and also the protein concentration in the bulk. Owing to the fact that we here only considered IRRAS spectra accumulated at a single incidence angle and polarization, the error margins are in the order of 50%. In future the analysis will be extended to a global analysis in which IRRAS spectra as well as absolute reflection spectra are included, acquired at various angles of incidence and both polarizations. This is to obtain a unique consistent fit and to minimize the error margins of the deduced layer thicknesses and concentrations, and more detailed information about the molecular properties of the proteins as for instance the orientation (reflected in the anisotropy of the complex refractive index). Also the number of stratified layers will be extended to allow a study of the molecular properties at different depths. Furthermore, the analysis need and will be extended to an iterative fit procedure for which the ATR and/or transmission spectrum as a first guess is used, in order to extract the extinction coefficient of the proteins and their conformation at the interface.

Acknowledgements We gratefully acknowledge the Laboratory of Physical Chemistry and Colloid Science of Wageningen University for letting us use the external reflection accessory, Ton Visser for stimulating discussions and Arne Gericke for introducing us to the field of IRRAS. The experiments comply with the current laws of the country in which the experiments are performed.

References

Atkinson PJ, Dickinson E, Horne DS, Richardson RM (1995) Neutron reflectivity of adsorbed β-casein and β-lactoglobulin at the air/water interface. J Chem Soc Faraday Trans 91: 2847–2854

Atkinson PJ, Dickinson E, Horne DS, Leermakers FAM, Richardson RM (1996) Theoretical and experimental investigations of adsorbed protein structure at a fluid interface. Ber Bunsenges Phys Chem 100: 994–998

Baekmark TR, Wiesenthal T, Kuhn P, Albersdorfer A, Nuyken O, Merkel R (1999) A systematic infrared reflection-absorption spectroscopy and film balance study of the phase behavior of lipopolymer monolayers at the air-water interface. Langmuir 15: 3616–3626

Bardwell JA, Dignam MJ (1985) Extensions of the Kramers-Kronig transformation that cover a wide range of practical spectroscopic applications. J Chem Phys 83: 5468–5478

Bechinger B, Ruysschaert JM, Goormaghtigh E (1999) Membrane helix orientation from linear dichroism of infrared attenuated total reflection spectra. Biophys J 76: 552–563

Berge B, Lenne PF, Renault A (1998) X-ray grazing incidence diffraction on monolayers at the surface of water. Curr Opin Colloid Interface Sci 3: 321–326

Bertie JE, Khalique Ahmed M, Eysel HH (1989) Infrared intensities of liquids. 5. Optical and dielectric constants, integrated intensities and dipole moment derivatives of H_2O and D_2O at 22 °C. J Chem Phys 93: 2210–2218

Blaudez D, Buffeteau T, Cornut JC, Desbat B, Escafre N, Pezolet M, Turlet JM (1993) Polarization-modulated FT-IR spectroscopy of a spread monolayer at the air/water interface. Appl Spectrosc 47: 869–874

Blaudez D, Buffeteau T, Cornut JC, Desbat B, Escafre N, Pezolet M, Turlet JM (1994) Polarized modulation FTIR spectroscopy at the air-water interface. Thin Solid Films 242: 146–150

Blaudez D, Turlet JM, Dufourcq J, Bard D, Buffeteau T, Desbat B (1996) Investigations at the air/water interface using polarization modulation IR spectroscopy. J Chem Soc Faraday Trans 92: 525–530

Blaudez D, Buffeteau T, Desbat B, Fournier P, Ritcey AM, Pezolet M (1998) Infrared reflection-absorption spectroscopy of thin organic films on nonmetallic substrates: optimal angle of incidence. J Phys Chem B 102: 99–105

Born MA, Wolf E (1975) Principles of optics. Pergamon Press, Oxford

Buffeteau T, Blaudez D, Pere E, Desbat B (1999) Optical constant determination in the infrared of uniaxially oriented monolayers from transmittance and reflectance measurements. J Phys Chem B 103: 5020–5027

Byler DM, Susi H (1986) Examination of the secondary structure of proteins by deconvolved FTIR spectra. Biopolymers 25: 469–487

Cornut I, Desbat B, Turlet JM, Dufourcq J (1996) In situ study by polarization modulated Fourier transform infrared spectroscopy of the structure and orientation of lipids and amphipathic peptides at the air-water interface. Biophys J 70: 305–312

Creighton TE (1996) Proteins in solution and in membranes. In: Creighton TE (ed) Proteins, structures and molecular properties. Freeman, New York, pp 262–266

Dickinson E, Horne DS, Phipps JS, Richardson RM (1993a) A neutron reflectivity study of the adsorption of β-casein at fluid interfaces. Langmuir 9: 242–248

Dickinson E, Horne DS, Richardson RM (1993b) Neutron reflectivity study of the competitive adsorption of beta-casein and water-soluble surfactant at the planar air-water interface. Food Hydrocolloids 7: 497–505

Dluhy RA (1986) Quantitative external reflection infrared spectroscopic analysis of insoluble monolayers spread at air-water interface. J Phys Chem 90: 1373–1379

Dluhy RA, Cornell DG (1985) In situ measurements of the infrared spectra of insoluble monolayers at the air-water interface. J Phys Chem 89: 3195–3197

Dluhy RA, Mitchell ML, Pettenski T, Beers J (1988) Design and interfacing of an automated Langmuir-type film balance to an FT-IR spectrometer. Appl Spectrosc 42: 1289–1293

Feijter JA de, Benjamins J, Veer FA (1978) Ellipsometry as a tool to study the adsorption behavior of synthetic and biopolymers at the air-water interface. Biopolymers 17: 1759–1772

Flach CR, Brauner JW, Taylor JW, Baldwin RC, Mendelsohn R (1994) External reflection FTIR of peptide monolayer films in situ at the air/water interface: experimental design, spectra-structure correlations and effects of hydrogen-deuterium exchange. Biophys J 67: 402–410

Flach CR, Prendergast FG, Mendelsohn R (1996) Infrared reflection-absorption of melittin interaction with phospholipid monolayers at the air/water interface. Biophys J 70: 539–546

Flach CR, Gericke A, Mendelsohn R (1997) Quantitative determination of molecular chain tilt angles in monolayer films at the air/water interface: infrared reflection/absorption spectroscopy of behenic acid methyl ester. J Phys Chem B 101: 58–65

Flach CR, Gericke A, Keough KMW, Mendelsohn R (1999) Palmitoylation of lung surfactant protein SP-C alters surface thermodynamics, but not protein secondary structure or orientation in 1,2-dipalmitoylphosphatidylcholine Langmuir films. Biochim Biophys Acta Biomembr 1416: 11–20

Gericke A, Hühnerfuss H (1993) In situ investigation of saturated long-chain fatty acids at the air/water interface by external reflection-absorption spectrometry. J Phys Chem 97: 12899–12908

Gericke A, Flach CR, Mendelsohn R (1997) Structure and orientation of lung surfactant SP-C and L-alpha-dipalmitoylphosphatidylcholine in aqueous monolayers. Biophys J 73: 492–499

Goormaghtigh E, Ruysschaert JM (1990) Polarized attenuated total reflection infrared spectroscopy as a tool to investigate the conformation and orientation of membrane components. In: Brasseur R (ed) Molecular description of biological membranes by computer-aided conformational analysis. CRC Press, Boca Raton, Fla., pp 285–329

Goormaghtigh E, Cabiaux V, Ruysschaert JM (1994) Determination of soluble and membrane protein structure by Fourier transform infrared spectroscopy. In: Hilderson HJ, Ralston GB (eds) Physicochemical methods in the study of biomembranes. Plenum Press, New York, pp 329–450

Harzallah B, Aguié-Béghin V, Douillard R, Bosio L (1998) A structural study of β-casein adsorbed layers at the air-water interface using X-ray and neutron reflectivity. Int J Biol Macromol 23: 73–84

Horne DS, Atkinson PJ, Dickinson E, Pinfield VJ, Richardson RM (1998) Neutron reflectivity study of competitive adsorption of beta-lactoglobulin and nonionic surfactant at the air-water interface. Int Dairy J 8:73–77

Jackson M, Mantsch HH (1995) The use and misuse of FTIR spectroscopy in the determination of protein structure. Crit Rev Biochem Mol Biol 30: 95–120

Jongh HHJ de, Goormaghtigh E, Ruysschaert JM (1995) Tertiary stability of native and methionine-80 modified cytochrome *c* detected by proton-deuterium exchange using on-line Fourier transform infrared spectroscopy. Biochemistry 34: 172–179

Jongh HHJ de, Goormaghtigh E, Ruysschaert JM (1997) Monitoring structural stability of trypsin inhibitor at the submolecular level by amide-proton exchange using Fourier transform infrared spectroscopy: a test case for more general application. Biochemistry 36: 13593–13602

Lu JR, Thomas RK (1998) Neutron reflection from wet interfaces. J Chem Soc Faraday Trans 94: 995–1018

Lu JR, Su TJ, Thomas RK, Penfold J, Webster J (1998) Structural conformation of lysozyme layers at the air/water interface studied by neutron reflection. J Chem Soc Faraday Trans 94: 3279–3287

Lu JR, Su TJ, Penfold J (1999) Adsorption of serum albumins at the air/water interface. Langmuir 15: 6975–6983

Ohta K, Ishida H (1988) Comparison among several numerical integration methods for Kramers-Kronig transformation. Appl Spectrosc 42: 952–957

Pastrana RB, Taneva S, Keough KMW, Mautone AJ, Mendelsohn R (1995) External reflection absorption infrared spectroscopy study of lung surfactant proteins SP-B and SP-C in phospholipid monolayers at the air/water interface. Biophys J 69: 2531–2540

Picard F, Buffeteau T, Desbat B, Auger M, Pezolet M (1999) Quantitative orientation measurements in thin lipid films by attenuated total reflection infrared spectroscopy. Biophys J 76: 539–551

Ren Y, Meuse CW, Hsu LS (1994) Reflectance infrared spectroscopic analysis of monolayer films at the air-water interface. J Phys Chem 98: 8424–8430

Ren Y, Shoichet MS, McCarthy TJ, Stidham HD, Hsu SL (1995) Spectroscopic characterization of polymer adsorption at the air-solution interface. Macromolecules 28: 358–364

Simon-Kutscher J, Gericke A, Hühnerfuss H (1996) Effect of bivalent Ba, Cu, Ni, and Zn cations on the structure of octadecanoic acid monolayers at the air-water interface as determined by external infrared reflection-absorption spectroscopy. Langmuir 12: 1027–1034

Ulrich WP, Vogel H (1999) Polarization-modulated FTIR spectroscopy of lipid/gramicidin monolayers at the air/water interface. Biophys J 76: 1639–1647

Wu F, Flach CR, Seaton BA, Mealy TR, Mendelsohn R (1999) Stability of annexin V in ternary complexes with Ca^{2+} and anionic phospholipids: IR studies of monolayer and bulk phases. Biochemistry 38: 792–799

Yamamoto K, Ishida H (1994) Optical theory applied to infrared spectroscopy. Vib Spectrosc 8: 1–36